

A novel fitted numerical scheme for time-fractional singularly perturbed convection-diffusion problems with a delay in time via cubic B -spline approach

Worku Tilahun Aniley, Gemechis File Duressa*

Department of Mathematics, Jimma University, Jimma, Ethiopia

Email(s): workutil12@gmail.com, gammeeef@gmail.com

Abstract. This paper presents a uniformly convergent numerical scheme for time-fractional singularly perturbed convection-diffusion problem with delay in time. The time-fractional derivative is considered in the Caputo sense and treated using the implicit Euler method. Then, a uniformly convergent numerical scheme based on cubic B -spline method is developed along the spatial direction. The technique is proved rigorously for parameter-uniform convergence. By a numerical experimentation, it is also validated that the computational result agrees with the theoretical expectation and it is also more accurate than some existing numerical methods.

Keywords: Time-fractional, convection-diffusion, uniformly convergent, cubic B -spline.

AMS Subject Classification 2010: 26A33, 65M06, 65M12.

1 Introduction

The study of fractional calculus has gotten much attention for the last few decades due to its wide application to model real life phenomenas such as fluid flow, finance model, heat model, temperature model, control model, gravitational model, statistics and probability, anomalous transport, rheology, diffusive transport akin to diffusion, electrical networking, electromagnetic theory, viscoelasticity, the electro chemistry of corrosion, and many other phenomenas [14].

For example, inspired by the aforementioned advantage of fractional calculus, the authors in [14] studied the famous mortgage model of economics numerically. First, the authors have formulated the proposed model in ordinary derivative form as follows. That is, they have assumed a client takes out a settled rate of mortgage for p dollars at an interest rate of R percent per year, with the month to month installment A , and need to pay off the credit in y years. Their main motive was to discover out what the

*Corresponding author

Received: 08 November 2023/ Revised: 03 December 2023/ Accepted: 16 December 2023

DOI: 10.22124/jmm.2023.25969.2303

yearly installment ought to be, so that the advance is cleared in y a long time. They obtained the model:

$$\begin{cases} \frac{dy(t)}{dt} = Ry(t) - A, \\ y(0) = p, \end{cases} \quad (1)$$

where A is monthly payment, R stands for interest rate, p initial taken amount in Dollars and y is the total amount of mortgage. Then, taking into account the advantage of fractional calculus, the authors took the model in Eq. (1), in fractional derivative form as:

$$\begin{cases} {}_0^C D_t^\gamma y(t) = Ry(t) - A, & 0 < \gamma \leq 1, \\ y(0) = p, \end{cases} \quad (2)$$

where ${}_0^C D_t^\gamma y(t)$ stands for the Caputo fractional derivative. Then, they have applied a shifted Legendre polynomials to reduce the proposed model to some algebraic type matrix equation and solved the model numerically for various fractional order of γ . From the numerical result, they have observed that the new proposed model, that is the fractional order model, has a better payment plan. Moreover, the authors also observed that smaller fractional order γ implies faster payment plan with lowest interest rate. Finally, the authors concluded that, the utilization of fractional differential equation strategy empowers a client to pay off loans more faster than integer order differential equation.

Fractional differential equation is a generalization of traditional integer order differential equation to a non-integer order called fractional order. In fact, currently scholars in different fields of science have arguing that fractional order differential equations are more suitable than integer order to model real life problems [11]. Finding the analytic solution of such differential equation is not trivial. Even if the analytical solution exist for some specific FDEs, they are communicated in terms of special functions which are difficult to asses. As a result, researchers are compelling to the numerical approach to establish an efficient approximate solution for FDEs [14]. The numerical methods in [8, 13, 19, 21, 22, 24, 27] are few of the most recently developed numerical methods for the approximate solution of FDEs.

Many real life phenomenas that display time-delayed or memory effect can be modeled by a partial differential equation with a delay term. Such differential equations occur in generic repression (taking into account time delays from processes of transcription and translation as well as spatial diffusion of reactants in the models), population ecology (to describe the interaction of spatial diffusion and time delays) and general control problems (where the controlled signal may be delayed in time because of the presence of time delays in actuation and in information transmission and processing) [18]. A delay partial differential equations are partial differential equations in which the highest order derivative term multiplied by a small perturbation parameter ε and having at least one delay term is called singularly perturbed delay partial differential equation. Currently, the study of such equation is attracting the focus of many researchers due to its application in diverse fields of science such as control theory, biosciences, economics, tumor growth, material science, neural networks, and robotics [10]. As a result, researchers have presented different numerical methods for solving such problems. The methods presented in [5, 12, 15–17, 23, 26] are few to list.

Solving time-fractional delay partial differential equation accurately and effectively is not trivial, because the evaluation of a dependent variable of such equation at any time t depends not only on its value at $t - \delta$ (for some delay δ) but also on all previous solutions. To alleviate such difficulties, researchers have been compelled to the numerical approach. For instance, a second order numerical

scheme is presented in [3] for the numerical solution of aforementioned problem. To developed the method, the authors considered the time-fractional derivative in the Caputo sense. Then, they have used Crank-Nicholson method to discretize the temporal direction and then applied a spline functions with a tension factor in the spatial direction. Choundhary et al. [2] also presented a second order numerical scheme for time-fractional partial differential equations with a delay in time. To develop the scheme, first the authors discretized the fractional derivative using a finite-difference scheme with second-order accuracy. Then, they have applied a cubic *B*-spline collocation method to get the full discretization.

A very less literature is available related to the numerical solution of time-fractional singularly perturbed PDEs with a delay in time and non-delay. Liu et al. [11] proposed a stabilized numerical method with high accuracy to solve time-fractional singularly perturbed convection-diffusion equation with variable coefficients. They have adopted the tailored finite point method (TFPM) to discrete equation in the spatial direction, while the time direction is discretized by the G-L approximation and the L_1 approximation. Kumar et al. [10] developed a stable finite difference method(SFDM) for time-fractional singularly perturbed convection-diffusion problems with a delay in time. The fractional derivative is considered in the Caputo sense. Then, the SFDM is constructed based on the stability of the analytical solution.

The main motive of this work is to develop an accurate and uniformly convergent numerical scheme for the time-fractional singularly perturbed problem with a delay in time of the form:

$$\begin{cases} \mathcal{L}_\varepsilon u(x,t) \equiv D_t^\gamma u(x,t) - \varepsilon u_{xx}(x,t) + p(x)u_x(x,t) + q(x,t)u(x,t) \\ \quad = -r(x,t)u(x,t - \delta) + g(x,t), \quad (x,t) \in \Omega, \\ u(x,t) = \psi(x,t), \quad \text{for } (x,t) \in [0,1] \times [-\delta,0], \\ u(0,t) = \phi(t), \quad u(1,t) = \varphi(t), \quad \text{for } t \in (0,T]. \end{cases} \quad (3)$$

where $\Omega = (0,1) \times (0,T]$, D_t^γ is the Caputo fractional derivative, δ is a delay parameter and ε is a positive constant satisfying $0 < \varepsilon \ll 1$. If $p(x) \geq p > 0$, $q(x,t) \geq 0$, $r(x,t) \geq \alpha > 0$ and $g(x,t)$ are smooth and bounded functions on the domain $\bar{\Omega}$ and the given initial data and boundary conditions are also smooth and bounded in their domain, then the solution of the model problem Eq. (3) exhibit a right boundary layer of width $O(\varepsilon)$.

Due to the presence of the singular perturbation parameter ε , all the classical numerical methods that are used to solve time-fractional PDEs fails to solve the considered problem. Hence, to develop the scheme, we have considered the time-fractional in the Caputo sense and discretized it using implicit Euler method. Then a collocation cubic B-spline method is applied along the spatial direction to obtain a fully discretized scheme. In order to control the effect of the perturbation parameter, artificial viscosity or fitting factor is introduced in to the scheme.

The remaining part of the manuscript is organized as follows. Section 2 comprises some preliminaries and properties of continuous solution. Section 3 deals with the numerical scheme. Rigorous uniform convergence analysis is presented in Section 4. In Section 5, numerical experimentation is carried out to prove the theoretical results. Finally, the paper ends with some observations, concluding remarks in Section 6.

2 Preliminaries and properties of continuous solution

Firstly, let us consider the following definition and estimates, which will be used herein.

Definition 1. The γ -order Caputo fractional derivative of a function $v(x, t)$ with respect to t , with lower limit zero is defined by:

$$D_0^\gamma v(x, t) = \frac{1}{\Gamma(1-\gamma)} \int_0^t \frac{\partial v(x, \tau)}{\partial \tau} (t-\tau)^{-\gamma} d\tau, \text{ for } 0 < \gamma < 1,$$

where $\Gamma(\cdot)$ is the gamma function.

The differential operator \mathcal{L}_ε in Eq. (3) satisfies the following continuous maximum principle.

Theorem 1. Let the function $\vartheta(x, t) \in C^2(\Omega) \cap C^0(\bar{\Omega})$ satisfies $\mathcal{L}\vartheta(x, t) \geq 0$, $\forall (x, t) \in \Omega$ and $\vartheta(x, t) \geq 0$, $\forall (x, t) \in \Gamma = \{0\} \times [0, T] \cup \{1\} \times [0, T] \cup [0, 1] \times [-\delta, 0]$. Then, we have $\vartheta(x, t) \geq 0$, $\forall (x, t) \in \bar{\Omega}$.

Proof. Consider a point (x^*, t^*) satisfying $\vartheta(x^*, t^*) = \min_{(x,t) \in \bar{\Omega}} \vartheta(x, t)$. Moreover, assume that $\vartheta(x^*, t^*) < 0$. Then, it is clear that $(x^*, t^*) \notin \Gamma$. But, from the theory of extrema of a function in calculus, we have $\vartheta_x(x^*, t^*) = 0$, $\vartheta_{xx}(x^*, t^*) \geq 0$ and $D_t^\gamma \vartheta(x, t) \leq 0$. Now, at the point of minimum (x^*, t^*) , we have:

$$\mathcal{L}_\varepsilon \vartheta(x, t) \equiv D_t^\gamma \vartheta(x^*, t^*) - \varepsilon \vartheta_{xx}(x^*, t^*) + p(x^*) \vartheta_x(x^*, t^*) + q(x^*) \vartheta(x^*, t^*) \leq 0,$$

which is a contradiction to the given hypothesis. Therefore, $\vartheta(x, t) \geq 0$, $\forall (x, t) \in \bar{\Omega}$. \square

The stability of the differential operator \mathcal{L}_ε and the ε -uniform boundedness for the solution of Eq. (3) is given by the following lemma.

Theorem 2. The ε -uniform bound on the solution of Eq. (3) satisfies the following bound:

$$\|u\| \leq \|u\|_\Gamma + \frac{\|\mathcal{L}_\varepsilon u\|}{p} \pm u(x, t).$$

Proof. Define the barrier function:

$$\vartheta(x, t) = \|u\|_\Gamma + \frac{\|\mathcal{L}_\varepsilon u\|}{p} \pm u(x, t), \quad (x, t) \in \bar{\Omega}.$$

Then, we have:

$$\vartheta(0, t) = \|u\|_\Gamma + \frac{\|\mathcal{L}_\varepsilon u\|}{p} \pm u(0, t) \geq \|u\|_\Gamma \pm u(0, t) \geq 0,$$

$$\vartheta(1, t) = \|u\|_\Gamma + \frac{\|\mathcal{L}_\varepsilon u\|}{p} \pm u(1, t) \geq \|u\|_\Gamma \pm u(1, t) \geq 0,$$

and also for $(x, t) \in [0, 1] \times [-\delta, 0]$,

$$\vartheta(x, t) = \|u\|_\Gamma + \frac{\|\mathcal{L}_\varepsilon u\|}{p} \pm u(x, t) \geq \|u\|_\Gamma \pm u(x, t) \geq 0.$$

Moreover, for $(x, t) \in \Omega$, we have

$$\begin{aligned} \mathcal{L}_\varepsilon \vartheta(x, t) &= p \left(\|u\|_\Gamma + \frac{\|\mathcal{L}_\varepsilon u\|}{p} \right) \pm \mathcal{L}_\varepsilon u(x, t) \\ &\geq p \|u\|_\Gamma + \|\mathcal{L}_\varepsilon u\| \pm \mathcal{L}_\varepsilon u(x, t) \\ &\geq \|\mathcal{L}_\varepsilon u\| \pm \mathcal{L}_\varepsilon u(x, t) \\ &\geq 0. \end{aligned}$$

Therefore, the application of the maximum principle in Theorem 1 ends the proof. \square

3 Formulation of the numerical scheme

3.1 Discretization along the temporal direction

First, we divide the time domain $[0, T]$ uniformly into N subintervals with uniform step size $\Delta t = T/N$. N is chosen in such a way that, $\delta = n\Delta t$ for some positive integer $n \in (0, N)$. Then, the set Ω^N is the collection of all mesh points in the time direction and it is given by:

$$\Omega^N = \{0 = t_0 < t_1 < t_2 < \dots < t_n = \delta < \dots < t_{N-1} < t_N = T\}.$$

The set of all mesh points from $-\delta$ to 0, Ω_δ^N , is also given by:

$$\Omega_\delta^N = \{t_{-n} = -\delta < t_{-n+1} < t_{-n+2} < \dots < t_{-1} < t_0 = 0\}.$$

Following the approach in [1, 20], the Caputo time-fractional derivative $D_t^\gamma u(x, t)$ at time $t = t_j$ is approximated by the following quadrature formula:

$$\begin{aligned} D_t^\gamma u(x, t_j) &= \frac{1}{\Gamma(1-\gamma)} \int_0^{t_j} \frac{\partial u(x, \tau)}{\partial \tau} (t_j - \tau)^{-\gamma} d\tau \\ &= \frac{1}{\Gamma(1-\gamma)} \sum_{k=0}^{j-1} \left(\frac{u(x, t_{k+1}) - u(x, t_k)}{\Delta t} \right) \int_{t_k}^{t_{k+1}} (t_j - \tau)^{-\gamma} d\tau + e_{\Delta t}^j \\ &= \frac{(\Delta t)^{-\gamma}}{\Gamma(2-\gamma)} \sum_{k=0}^{j-1} b_k \left(u(x, t_{j-k}) - u(x, t_{j-k-1}) \right) + e_{\Delta t}^j. \end{aligned}$$

Hence,

$$D_t^\gamma u(x, t_j) = \beta \sum_{k=0}^{j-1} b_k \left(u(x, t_{j-k}) - u(x, t_{j-k-1}) \right) + e_{\Delta t}^j, \tag{4}$$

where, $\beta = \frac{(\Delta t)^{-\gamma}}{\Gamma(2-\gamma)}$, $e_{\Delta t}^j = \frac{(\Delta t)}{\Gamma(1-\gamma)} \sum_{k=0}^{j-1} \int_{t_k}^{t_{k+1}} (t_j - \tau)^{-\gamma} d\tau$, $b_k = \left((k+1)^{1-\gamma} - (k)^{1-\gamma} \right)$.

Lemma 1. The local truncation error $e_{\Delta t}^j$ in Eq. (4) is bounded. $|e_{\Delta t}^j| \leq C(\Delta t)^{2-\gamma}$.

Using Eq. (4) into Eq. (3) and rearranging, we obtain the semi-discrete problem:

$$\begin{cases} \overline{\mathcal{L}}_\varepsilon U(x, t_j) \equiv -\varepsilon U_{xx}(x, t_j) + p(x)U_x(x, t_j) + Q(x, t_j)U(x, t_j) = R(x, t_j), \\ U(x, t_j) = \psi(x, t_j), & \text{for } (x, t_j) \in [0, 1] \times \Omega_\delta^N, \\ U(0, t_j) = \phi(t_j), \quad U(1, t_j) = \varphi(t_j), & \text{for } t_j \in \Omega^N. \end{cases} \tag{5}$$

where,

$$\begin{aligned} Q(x, t_j) &= q(x, t_j) + \beta, \\ R(x, t_j) &= -r(x, t_j)U(x, t_{j-n}) + g(x, t_j) + \beta U(x, t_{j-1}) - \beta \sum_{k=1}^{j-1} b_k \left(U(x, t_{j-k}) - U(x, t_{j-k-1}) \right). \end{aligned}$$

In particular, we can rewrite $R(x, t_j)$ as:

$$R(x, t_j) = \begin{cases} -r(x, t_j)\psi(x, t_j) + g(x, t_j) + \beta U(x, t_{j-1}) - \beta \sum_{k=1}^{j-1} b_k \left(U(x, t_{j-k}) - U(x, t_{j-k-1}) \right), & \text{for } j = 1, 2, 3, \dots, n, \\ -r(x, t_j)U(x, t_{j-n}) + g(x, t_j) + \beta U(x, t_{j-1}) - \beta \sum_{k=1}^{j-1} b_k \left(U(x, t_{j-k}) - U(x, t_{j-k-1}) \right), & \text{for } j = n+1, n+2, \dots, N. \end{cases}$$

Lemma 2 ([9, 10]). *The solution $U(x, t_j)$ of the semi-discrete scheme in Eq. (5) and its derivatives satisfies the following bound.*

$$\left| \frac{d^k U(x, t_j)}{dx^k} \right| \leq C \left(1 + \varepsilon^{-i} \exp(-p(1-x)/\varepsilon) \right), \quad \text{for } k = 0, 1, 2, 3, 4.$$

Using the approach in [4], the asymptotic expansion for the solution of the problem in Eq. (5) can be expressed as:

$$U(x) = U_0(x) + \frac{P(1)U_0(1)}{P(x)} \exp \left(\int_x^1 - \left(\frac{P^2(s) + \varepsilon Q(s)}{\varepsilon P(s)} \right) ds \right) + O(\varepsilon).$$

Using Taylor series expansion for $P(x)$ and $Q(x)$ about '1' and restricting to their first term gives:

$$U(x) = U_0(x) + U_0(1) \exp \left(- \frac{(P^2(1) + \varepsilon Q(1))(1-x)}{\varepsilon P(1)} \right) + O(\varepsilon). \quad (6)$$

3.2 Discretization along the spatial direction

Here, we use a cubic B -spline collocation method in order to solve the singularly perturbed problem in Eq. (5) by introducing a fitting factor. Let $\pi = \{a = x_0 < x_1 < x_2 < \dots < x_{M-1} < x_M = b\}$ be a uniform partition of the interval $[0, 1]$ such that $h = \frac{b-a}{M}$. Then, a cubic B -spline ($B_i(x)$) at point π can be defined as:

$$B_i(x) = \frac{1}{h^3} \begin{cases} (x - x_{i-2})^3, & \text{if } x_{i-2} \leq x < x_{i-1}, \\ -3(x - x_{i-1})^3 + 3h(x - x_{i-1})^2 + 3h^2(x - x_{i-1}) + h^3, & \text{if } x_{i-1} \leq x < x_i, \\ -3(x_{i+1} - x)^3 + 3h(x_{i+1} - x)^2 + 3h^2(x_{i+1} - x) + h^3, & \text{if } x_i \leq x < x_{i+1}, \\ (x_{i+2} - x)^3, & \text{if } x_{i+1} \leq x < x_{i+2}, \\ 0, & \text{otherwise.} \end{cases} \quad (7)$$

From Eq. (7), it is trivial to check that each of the spline $B_i(x)$ is twice continuously differentiable on the entire real line. Let $\Lambda = \{B_{-1}, B_0, B_1, \dots, B_{M+1}\}$ and $\Phi_3(\pi) = \text{span}(\Lambda)$. Then, the functions B_i 's are linearly independent on $[0, 1]$ and thus $\Phi_3(\pi)$ is $N+3$ dimensional. Now, we approximate the solution $U(x, t_j)$ by $S(x, t_j)$ in the form:

$$S(x) = \sum_{i=-1}^{i=M+1} \alpha_i B_i(x), \quad (8)$$

where α_i 's are unknown real coefficients, called degree of freedom, to be determined.

Using the approximation in Eq. (8), at the nodal point x_i , Eq. (5) becomes:

$$-\varepsilon\left(\frac{6}{h^2}(\alpha_{i-1} - 2\alpha_i + \alpha_{i+1})\right) + P_i\left(\frac{3}{h}(\alpha_{i+1} - \alpha_{i-1})\right) + Q_i(\alpha_{i-1} + 4\alpha_i + \alpha_{i+1}) = R_i. \quad (9)$$

To control the effect of the singular perturbation parameter on the solution behavior, we introduce the artificial viscosity $\sigma(x_i, \varepsilon)$ on Eq. (9) and after rearrangement we obtain:

$$\left(\frac{-6\sigma_i}{h} - 3P_i + hQ_i\right)\alpha_{i-1} + \left(\frac{12\sigma_i}{h} + 4hQ_i\right)\alpha_i + \left(\frac{-6\sigma_i}{h} + 3P_i + hQ_i\right)\alpha_{i+1} = hR_i, \quad (10)$$

where, $\sigma(x_i, \varepsilon) = \sigma_i$ is the artificial viscosity which is to be determined in such away that the solution of Eq. (10) converges uniformly to the exact solution of Eq. (3).

3.2.1 Design of artificial viscosity

Taking the limiting case $h \rightarrow 0$ of Eq. (10) and Eq. (6), respectively gives:

$$\lim_{h \rightarrow 0} \frac{\sigma_i}{h} = \frac{p_0}{2} \left(\frac{\alpha_{i+1} - \alpha_{i-1}}{\alpha_{i-1} - 2\alpha_i + \alpha_{i+1}} \right),$$

and

$$\alpha_{i-1} + 4\alpha_i + \alpha_{i+1} = U_0(0) + U_0(1) \exp\left(-\frac{(P^2(1) + \varepsilon Q(1))\left(\frac{1}{\varepsilon} - i\rho\right)}{P(1)}\right),$$

where $\rho = \frac{h}{\varepsilon}$. Now, evaluating the values of $\lim_{h \rightarrow 0} \frac{\sigma_i}{h}$ at the nodal points x_{i-1} , x_i and x_{i+1} and adding in the proportion 1, 4, 1 respectively and eliminating the α_i 's gives:

$$\sigma_i = \frac{\varepsilon \rho P_i}{2} \coth\left(\frac{\rho P_i}{2}\right).$$

Following the approach in [4], we obtain:

$$|\sigma_i - \varepsilon| \leq C \left(\frac{h^2}{\varepsilon + h} \right). \quad (11)$$

Now, we can rewrite Eq. (10) in a three term recurrence relation as:

$$E_i \alpha_{i-1} + F_i \alpha_i + G_i \alpha_{i+1} = H_i, \quad i = 0, 1, 2, 3, \dots, M, \quad (12)$$

where

$$\begin{aligned} E_i &= -6\sigma_i - 3hP_i + h^2Q_i, \\ F_i &= 12\sigma_i + 4h^2Q_i, \\ G_i &= -6\sigma_i + 3hP_i + h^2Q_i, \\ H_i &= h^2R_i. \end{aligned}$$

From the boundary conditions we obtain:

$$\begin{aligned} \alpha_{-1} &= \phi(t_j) - 4\alpha_0 - \alpha_1, \\ \alpha_{M+1} &= \varphi(t_j) - \alpha_{M-1} - 4\alpha_M. \end{aligned} \tag{13}$$

Using Eq. (13) into Eq. (12), we have:

$$\begin{aligned} (F_0 - 4E_0)\alpha_0 + (G_0 - E_0)\alpha_1 &= H_0 - E_0\phi(t_j), \\ (E_M - G_M)\alpha_{M-1} + (F_M - 4G_M)\alpha_M &= H_M - \varphi(t_j)G_M. \end{aligned} \tag{14}$$

From Eq. (12) and Eq. (14), we obtain the following $(N + 1) \times (N + 1)$ system of linear equations:

$$\begin{cases} (F_0 - 4E_0)\alpha_0 + (G_0 - E_0)\alpha_1 = H_0 - E_0\psi_1(0), & \text{for } i = 0 \\ E_i\alpha_{i-1} + F_i\alpha_i + G_i\alpha_{i+1} = H_i, & \text{for } i = 1, 2, 3, \dots, M - 1, \\ (E_M - G_M)\alpha_{M-1} + (F_M - 4G_M)\alpha_M = H_M - \psi_2(1)G_M, & \text{for } i = M. \end{cases} \tag{15}$$

The system of linear equations in Eq. (15) can be rewritten in a matrix form as:

$$A\alpha = H, \tag{16}$$

where $\alpha = (\alpha_0, \alpha_1, \alpha_2, \dots, \alpha_M)^t$,

$$A = \begin{bmatrix} F_0 - 4E_0 & G_0 - E_0 & 0 & 0 & 0 & \dots & 0 & 0 & 0 \\ E_1 & F_1 & G_1 & 0 & 0 & \dots & 0 & 0 & 0 \\ 0 & E_2 & F_2 & G_2 & 0 & \dots & 0 & 0 & 0 \\ 0 & 0 & E_3 & F_3 & G_3 & \dots & 0 & 0 & 0 \\ \vdots & \vdots \\ 0 & 0 & 0 & 0 & 0 & \dots & E_{M-1} & E_{M-1} & E_{M-1} \\ 0 & 0 & 0 & 0 & 0 & \dots & 0 & E_M - G_M & F_M - 4G_M \end{bmatrix},$$

and

$$H = [h^2R_0 - E_0\phi(t_j), H_1, H_2, H_3, \dots, H_{M_1}, h^2R_M - G_M\varphi(t_j)]^t.$$

For sufficiently small values of h , the coefficient matrix A is strictly diagonally dominant and hence nonsingular [7]. Since the coefficient matrix A is invertible, we can solve Eq. (16) for $\alpha_0, \alpha_1, \alpha_2, \dots, \alpha_M$ and substituting these values into Eq. (8), we can obtain the required approximate solution.

4 Convergence analysis

Lemma 3 ([4,7]). *The set of B-splines $\{B_{-1}, B_0, B_1, \dots, B_{M+1}\}$ defined by the relations in Eq. (7) satisfies the following inequality:*

$$\sum_{i=-1}^{i=M+1} |B_i(x)| \leq 10, \quad \text{for } 0 \leq x \leq 1.$$

Theorem 3. Let $S(x)$ be the collocation approximation from the spaces of cubic splines to the solution $U(x)$ of the ordinary differential equation Eq. (5) at $(j)^{th}$ time level. If $R \in C^2[0, 1]$, then, the parameter uniform error estimate is given by:

$$\sup_{0 < \varepsilon \leq 1} \max_{0 \leq i \leq M} \|U(x_i) - S(x_i)\| \leq C \left(\frac{h^2}{\varepsilon + h} \right),$$

where C is a positive constant independent of ε and M .

Proof. Let $Y(x)$ be the unique spline that interpolate $U(x)$ to the solution of the semi-discrete problem Eq. (5) as:

$$Y(x) = \sum_{i=-1}^{i=M+1} \hat{\alpha}_i B_i(x). \tag{17}$$

If $R(x) \in C^2[0, 1]$, then $U(x_i) \in C^4[0, 1]$. Using the approach in [6], the error estimate becomes:

$$\|D^{(r)}(U(x) - Y(x))\| \leq \eta_i \|U^{(4)}\| h^{4-r}, \quad r = 0, 1, 2, \tag{18}$$

where η_i are constants. Assume $\widehat{L}S(x_i) = LU(x_i) = R(x_i)$ and $\widehat{L}Y(x_i) = \widehat{R}(x_i)$, $\forall i = 0, 1, 2, 3, \dots, M$, with the boundary conditions $Y(x_0) = \phi(x_0)$ and $Y(x_M) = \varphi(x_M)$. From the estimate in Eq. (18), we get:

$$\begin{aligned} |\widehat{L}S(x_i) - \widehat{L}Y(x_i)| &= \|LU(x_i) - \widehat{L}Y(x_i)\|, \\ &\leq |\sigma_i - \varepsilon| U^{(2)}(x_i) + \left(|\sigma_i| \eta_2 h^2 + \|p\| \eta_1 h^3 + \|Q\| \eta_0 h^4 \right) |U^{(2)}(x)|. \end{aligned}$$

Applying Eq. (11) and Lemma 2, we have:

$$|\widehat{L}U(x_i) - \widehat{L}Y(x_i)| \leq C \left(\frac{h^2}{\varepsilon + h} \right). \tag{19}$$

Using Eq. (16), the relation $\widehat{L}(U(x_i) - Y(x_i))$ leads to the linear system:

$$A(\alpha - \hat{\alpha}) = H - \widehat{H}, \tag{20}$$

where

$$\begin{aligned} \alpha - \hat{\alpha} &= (\alpha_0 - \hat{\alpha}_0, \alpha_1 - \hat{\alpha}_1, \dots, \alpha_M - \hat{\alpha}_M)^t, \\ H - \widehat{H} &= \left(h^2(H(x_0) - \widehat{H}(x_0)), h^2(H(x_1) - \widehat{H}(x_1)), \dots, h^2(H(x_M) - \widehat{H}(x_M)) \right)^t. \end{aligned}$$

Using the relation Eq. (19), we have:

$$\|H - \widehat{H}\| \leq C \left(\frac{h^4}{\varepsilon + h} \right). \tag{21}$$

On the other hand, for sufficiently small value of h , the coefficient matrix A of the system in Eq. (16) is strictly diagonally dominant and so that it is invertible [7]. Following the approach in [25], we have:

$$\|A^{-1}\| \leq \frac{C}{h^2}. \tag{22}$$

Using the relation Eq. (20), Eq. (21) and Eq. (22), we obtain:

$$|\alpha_i - \hat{\alpha}_i| \leq C \left(\frac{h^2}{\varepsilon + h} \right), \quad 0 \leq i \leq M. \quad (23)$$

Using the relations in Eq. (13), the estimates $|\alpha_{-1} - \hat{\alpha}_{-1}|$ and $|\alpha_{M+1} - \hat{\alpha}_{M+1}|$ are given by:

$$|\alpha_{-1} - \hat{\alpha}_{-1}| \leq C \left(\frac{h^2}{\varepsilon + h} \right) \quad \text{and} \quad |\alpha_{M+1} - \hat{\alpha}_{M+1}| \leq C \left(\frac{h^2}{\varepsilon + h} \right). \quad (24)$$

Hence, from equations Eq. (23) and Eq. (24), we obtain:

$$\max_{-1 \leq i \leq M+1} |\alpha_i - \hat{\alpha}_i| \leq C \left(\frac{h^2}{\varepsilon + h} \right). \quad (25)$$

Now, using the inequality Eq. (25) and Lemma 3, we have:

$$|S(x) - Y(x)| \leq \sum_{i=-1}^{M+1} (|\alpha_i - \hat{\alpha}_i|) |B_i(x)| \leq \max_{-1 \leq i \leq M+1} |\alpha_i - \hat{\alpha}_i| \sum_{i=-1}^{M+1} |B_i(x)| \leq C \left(\frac{h^2}{\varepsilon + h} \right).$$

Therefore, using triangular inequality, we obtain:

$$\sup_{0 < \varepsilon \leq 1} \max_{0 \leq i \leq M} \|U(x_i) - S(x_i)\| \leq C \left(\frac{h^2}{\varepsilon + h} \right). \quad \square$$

Theorem 4. Let $S(x)$ be the approximation to the solution $u(x, t)$ of the problem Eq. (3) at j^{th} time level of the fully discretized scheme after the temporal discretization. Then, the ε -uniform error estimate is given by:

$$\|u(x_i, t_j) - S(x_i)\| \leq C \left((\Delta t)^{2-\gamma} + \frac{h^2}{\varepsilon + h} \right).$$

Proof. The proof of this Theorem follows from the result of Lemma 1 and Theorem 3. □

5 Numerical result and discussion

Next, two model examples are considered to validate the main result of proposed method. Since the exact solution of the considered examples is not known, double mesh principle is applied to compute the maximum point wise error. That is,

$$E_\varepsilon^{M,N} = \max_{0 \leq i, j \leq M, N} \left| U^{M,N}(x_i, t_j) - U^{2M,2N}(x_{2i}, t_{2j}) \right|,$$

and the ε -uniform error is calculated using the formula

$$E_\varepsilon^{M,N} = \max_\varepsilon (E_\varepsilon^{M,N}).$$

The rate of convergence the proposed method is also found by:

$$R_\varepsilon^{M,N} = \frac{\log(E_\varepsilon^{M,N}) - \log(E_\varepsilon^{2M,2N})}{\log 2}.$$

Table 1: Comparison of maximum error for Example 1 for different values of γ with a fixed $\varepsilon = 2^{-10}$.

$\gamma \downarrow (M, N) \rightarrow$	(16, 20)	(32, 40)	(64, 80)	(128, 160)
Present Method				
0.25	6.1306e-03	3.3465e-03	1.7288e-03	8.6138e-04
0.5	6.3957e-03	3.4952e-03	1.8057e-03	8.9942e-04
0.75	6.8197e-03	3.7400e-03	1.9349e-03	9.6385e-04
Result in [10]				
0.25	1.1726e-02	6.3654e-02	3.3194e-02	1.6943e-03
0.5	1.2246e-02	6.6457e-03	3.4625e-03	1.7661e-03
0.75	1.3012e-02	7.0750e-03	3.6857e-03	1.8785e-03

Similarly, the uniform rate of convergence is found by:

$$R^{M,N} = \frac{\log(E^{M,N}) - \log(E^{2M,2N})}{\log 2}.$$

Example 1. Consider the time-fractional singularly perturbed problem:

$$\begin{cases} D^\gamma u(x,t) - \varepsilon u_{xx}(x,t) + (2-x^2)u_x(x,t) + (x+1)(t+1)u(x,t) = u(x,t-1) + 10t^2 \exp(-t)x(1-x), & \text{for } (x,t) \in (0,1) \times (0,2], \\ u(x,t) = 0, & \text{for } (x,t) \in [0,1] \times [-1,0], \\ u(0,t) = 0, \quad u(1,t) = 0, & \text{for } t \in [0,2]. \end{cases}$$

Example 2. Consider the time-fractional singularly perturbed problem:

$$\begin{cases} D^\gamma u(x,t) - \varepsilon u_{xx}(x,t) + (2-x^2)u_x(x,t) + xu(x,t) = u(x,t-1) + 10t^2 \exp(-t)x(1-x), & \text{for } (x,t) \in (0,1) \times (0,2], \\ u(x,t) = 0, & \text{for } (x,t) \in [0,1] \times [-1,0], \\ u(0,t) = 0, \quad u(1,t) = 0, & \text{for } t \in [0,2]. \end{cases}$$

The comparison of maximum absolute error of the proposed method with the method presented in [10] of Example 1 and Example 2, for different values of γ and a fixed $\varepsilon = 2^{-10}$ is presented in Table 1 and Table 4, respectively. The result in the two tables depict that the proposed method is more accurate than the method presented in [10]. Moreover, from the two tables, we can clearly observe that, as γ decreases the maximum absolute error also decreases depicting that fractional order models represent real life problems better than integer order model. The numerical result in Table 2 and Table 5 also indicates the comparison of maximum absolute error for Example 1 and Example 2 for different values of ε and a fixed $\gamma = 0.5$. From the result in these tables, we can observe that, the proposed scheme is more accurate than the method found in the literature. Table 3 and Table 6 shows the maximum absolute error of Example 1 and Example 2, for different values of ε and a fixed γ . The numerical result in these tables indicates, along each column, as the perturbation parameter goes smaller and smaller, the maximum absolute error of the proposed method becomes stable and identical after showing some grow up. This shows that, the proposed method is ε -uniform or uniformly convergent. Again, from the

Table 2: Comparison of maximum absolute error for Example 1 for different values of ε with a fixed $\gamma = 0.5$.

$\varepsilon^{-k} \downarrow / (M, N) \rightarrow$	(16,20)	(32,40)	(64,80)	(128,160)
Present method				
$k = 6$	5.5483e-03	1.8811e-03	5.2329e-04	1.3608e-04
$k = 10$	6.3957e-03	3.4952e-03	1.8057e-03	8.9942e-04
$k = 15$	6.3957e-03	3.4952e-03	1.8059e-03	9.1441e-04
$k = 20$	6.3957e-03	3.4952e-03	1.8059e-03	9.1441e-04
$k = 25$	6.3957e-03	3.4952e-03	1.8059e-03	9.1441e-04
Result in [10]				
$k = 6$	1.0088e-02	4.9401e-03	2.0143e-03	7.1385e-04
$k = 10$	1.2246e-02	6.6457e-03	3.4625e-03	1.7661e-03
$k = 15$	1.2361e-02	6.7337e-03	3.5212e-03	1.8011e-03
$k = 20$	1.2365e-02	6.7364e-03	3.5230e-03	1.8022e-03
$k = 25$	1.2365e-02	6.7364e-03	3.5230e-03	1.8022e-03

Table 3: Maximum absolute error, uniform error and uniform rate of convergence of Example 1 for different values of ε and a fixed $\gamma = 0.5$.

$\varepsilon \downarrow$	$M = 16$ $N = 16$	$M = 32$ $N = 32$	$M = 64$ $N = 64$	$M = 128$ $N = 128$	$M = 256$ $N = 256$
2^0	2.0830e-04	5.4976e-05	1.4724e-05	5.0331e-06	1.8480e-06
2^{-2}	5.2744e-04	1.4256e-04	4.5475e-05	1.6970e-05	6.2155e-06
2^{-4}	1.8635e-03	4.9464e-04	1.3029e-04	3.4376e-05	9.5567e-06
2^{-6}	5.5826e-03	1.8938e-03	5.2811e-04	1.3784e-04	3.5379e-05
2^{-8}	6.4298e-03	3.4650e-03	1.4976e-03	4.9702e-04	1.3749e-04
2^{-10}	6.4301e-03	3.5075e-03	1.8105e-03	9.0115e-04	3.8342e-04
2^{-12}	6.4301e-03	3.5075e-03	1.8107e-03	9.1613e-04	4.6001e-04
2^{-14}	6.4301e-03	3.5075e-03	1.8107e-03	9.1613e-04	4.6010e-04
2^{-16}	6.4301e-03	3.5075e-03	1.8107e-03	9.1613e-04	4.6010e-04
2^{-18}	6.4301e-03	3.5075e-03	1.8107e-03	9.1613e-04	4.6010e-04
2^{-20}	6.4301e-03	3.5075e-03	1.8107e-03	9.1613e-04	4.6010e-04
2^{-22}	6.4301e-03	3.5075e-03	1.8107e-03	9.1613e-04	4.6010e-04
2^{-24}	6.4301e-03	3.5075e-03	1.8107e-03	9.1613e-04	4.6010e-04
$E^{M,N}$	6.4301e-03	3.5075e-03	1.8107e-03	9.1613e-04	4.6010e-04
$R^{N,M}$	0.8744	0.9539	0.9829	0.9936	-

Table 4: Comparison of maximum error for Example 2 for different values of γ with a fixed $\varepsilon = 2^{-10}$.

$\gamma \downarrow (M, N) \rightarrow$	(16,20)	(32,40)	(64,80)	(128,160)
Present Method				
0.25	7.8363e-03	4.3838e-03	2.3386e-03	1.2274e-03
0.5	8.2620e-03	4.6158e-03	2.4763e-03	1.2971e-03
0.75	8.7558e-03	4.8891e-03	2.7152e-03	1.4216e-03
Result in [10]				
0.25	2.3562e-02	1.0942e-02	5.2006e-03	2.5142e-03
0.5	2.4877e-02	1.1527e-02	5.4771e-03	2.6471e-03
0.75	2.6875e-02	1.2479e-02	5.9366e-03	2.8698e-03

Table 5: Comparison of maximum error for Example 2 for different values of ϵ with a fixed $\gamma = 0.5$.

$\epsilon^{-k} \downarrow / (M, N) \rightarrow$	(16,20)	(32,40)	(64,80)	(128,160)
Present method				
$k = 6$	7.9095e-03	3.4200e-03	1.0661e-03	2.8417e-04
$k = 10$	8.2620e-03	4.6158e-03	2.4763e-03	1.2971e-03
$k = 15$	8.2620e-03	4.6158e-03	2.4768e-03	1.3265e-03
$k = 20$	8.2620e-03	4.6158e-03	2.4768e-03	1.3265e-03
$k = 25$	8.2620e-03	4.6158e-03	2.4768e-03	1.3265e-03
Result in [10]				
$k = 6$	1.5818e-02	7.8811e-03	2.9140e-03	8.1121e-04
$k = 10$	2.4877e-02	1.1527e-02	5.4771e-03	2.6471e-03
$k = 15$	2.6031e-02	1.2234e-02	5.8929e-03	2.8856e-03
$k = 20$	2.6068e-02	1.2257e-02	5.9063e-03	2.8933e-03
$k = 25$	2.6069e-02	1.2258e-02	5.9068e-03	2.8935e-03

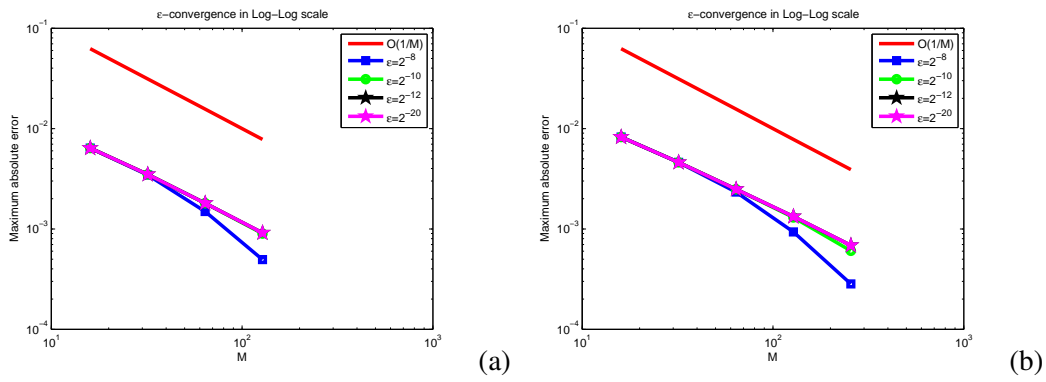


Figure 1: Log-log plot of the maximum absolute error (a) for Example 1 and (b) for Example 2.

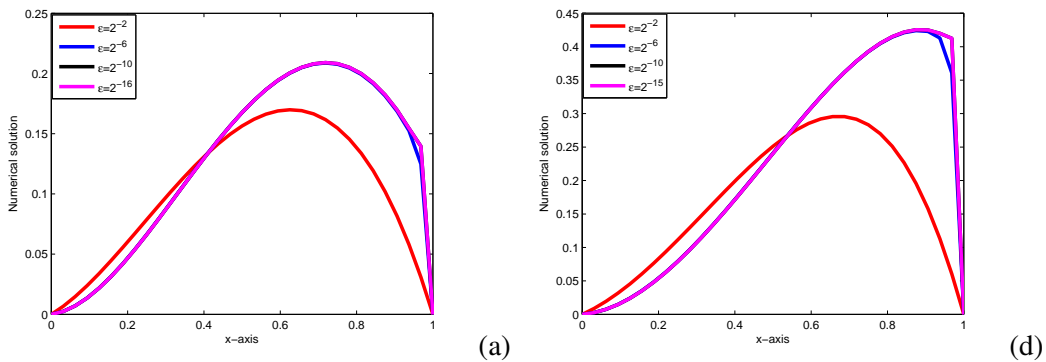


Figure 2: Boundary layer formation, (a) for Example 1 and (b) for Example 2 for various value of ϵ , $\gamma = 0.5$, $M = 32$ and $N = 40$.

last rows of these table, the proposed scheme is first order convergent which is in agreement with the theoretical expectation as it is indicated in Figure 1.

Table 6: Maximum absolute error, uniform error and uniform rate of convergence of Example 2 for different values of ϵ and a fixed $\gamma = 0.5$.

$\epsilon \downarrow$	$M = 16$ $N = 16$	$M = 32$ $N = 32$	$M = 64$ $N = 64$	$M = 128$ $N = 128$	$M = 256$ $N = 256$
2^0	3.6173e-04	9.4544e-05	2.5064e-05	6.7713e-06	2.1758e-06
2^{-2}	1.2161e-03	3.2236e-04	8.7236e-05	2.4172e-05	8.4533e-06
2^{-4}	3.6992e-03	9.5636e-04	2.4884e-04	6.6107e-05	1.7844e-05
2^{-6}	7.8879e-03	3.4133e-03	1.0639e-03	2.8340e-04	7.1822e-05
2^{-8}	8.2403e-03	4.6052e-03	2.3304e-03	9.3351e-04	2.8362e-04
2^{-10}	8.2403e-03	4.6091e-03	2.4871e-03	1.3013e-03	6.0621e-04
2^{-12}	8.2403e-03	4.6091e-03	2.4875e-03	1.3308e-03	6.8713e-04
2^{-14}	8.2403e-03	4.6091e-03	2.4875e-03	1.3308e-03	6.8730e-04
2^{-16}	8.2403e-03	4.6091e-03	2.4875e-03	1.3308e-03	6.8730e-04
2^{-18}	8.2403e-03	4.6091e-03	2.4875e-03	1.3308e-03	6.8730e-04
2^{-20}	8.2403e-03	4.6091e-03	2.4875e-03	1.3308e-03	6.8730e-04
2^{-22}	8.2403e-03	4.6091e-03	2.4875e-03	1.3308e-03	6.8730e-04
2^{-24}	8.2403e-03	4.6091e-03	2.4875e-03	1.3308e-03	6.8730e-04
$E^{M,N}$	8.2403e-03	4.6091e-03	2.4875e-03	1.3308e-03	6.8730e-04
$R^{N,M}$	0.8382	0.8898	0.9024	0.9533	-

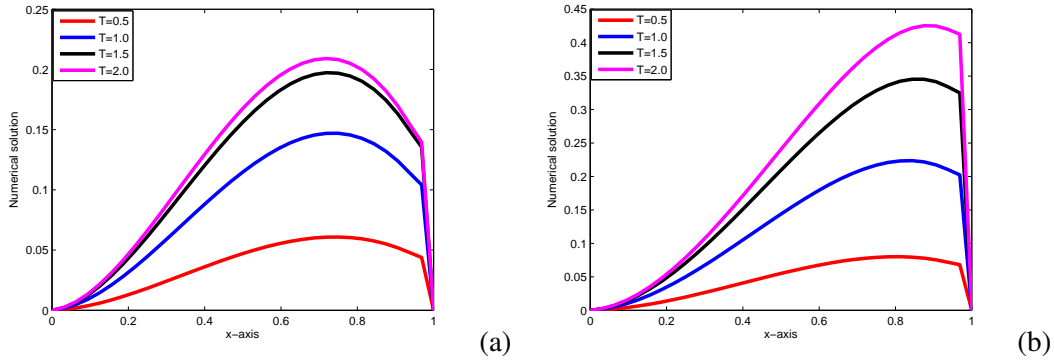


Figure 3: Line plot of Example 1 and 2, respectively for $\epsilon = 2^{-10}$, $\gamma = 0.5$, $M = 32$ and $N = 40$ at different time level by taking $t = 2$.

As one observes from Figures 2 (a) and (b), a strong right boundary layer is formed as the perturbation parameter ϵ becomes smaller and smaller. In this problem, the temporal delay parameter do not have any effect on the position and size of the boundary layer, as the layer is formed along the spatial direction. Figures 3 (a) and (b) shows a line plot of Example 1 and Example 2, respectively at different time level, for $\epsilon = 2^{-10}$, $\gamma = 0.5$, $M = 32$, $N = 40$ by taking $T = 2$. Figure 4 (a), (b) and (d) shows the the solution profile of Example 1 with a boundary layer formation for $\epsilon = 2^{-6}$, $\epsilon = 2^{-16}$, $M = 32$, $N = 40$ and $\gamma = 0.5$. Figure 5 (a), (b) shows the solution profile of Example 2 with a boundary layer formation for $\epsilon = 2^{-6}$, $\epsilon = 2^{-16}$, $M = 32$, $N = 40$ and $\gamma = 0.5$. From the figures, one can observe that the numerical solution of the governing problem forms a strong right boundary layer as the perturbation

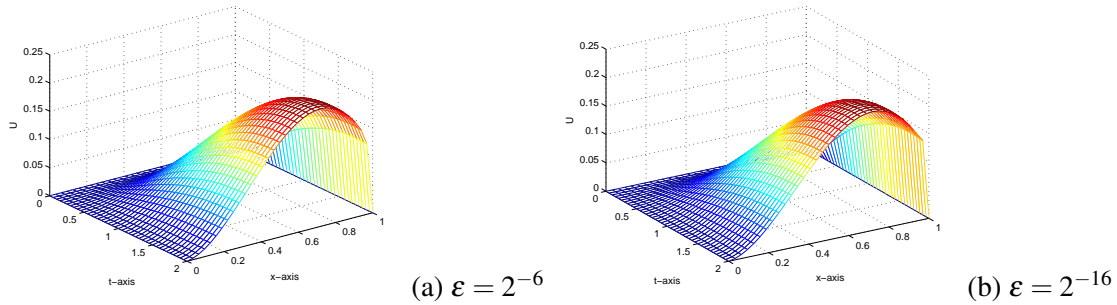


Figure 4: Numerical solution of Example 1 for various of ε with $\gamma = 0.5$, $M = 32$ and $N = 40$.

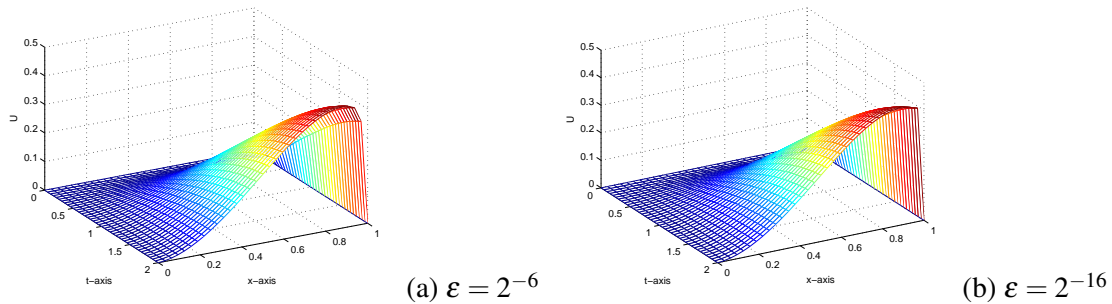


Figure 5: Numerical solution of Example 2 for various of ε with $\gamma = 0.5$, $M = 32$ and $N = 40$.

becomes smaller and smaller.

6 Conclusion

In this work, ε -uniform numerical method is presented to solve time-fractional singularly perturbed convection-diffusion problem with a delay in time. The time-fractional derivative is considered in a Caputo sense. Then, implicit Euler method is applied to discretized the temporal direction and then cubic B-splines techniques ia applied to solve the resulting system of ordinary differential equation in the spatial direction. In order to control the effect of the perturbation parameter, artificial viscosity or fitted factor is introduced to the problem. The ε -uniform convergence of the proposed method rigorously proved and shown to be accurate of order $O\left((\Delta t)^{2-\gamma} + \frac{h^2}{\varepsilon+h}\right)$. Two model examples are considered to test the validity of the proposed method. The numerical results show that the presented method provides more accurate solution than some recent existing methods.

References

- [1] W.T. Aniley, G.F. Duressa, *Uniformly convergent numerical method for time-fractional convection-diffusion equation with variable coefficients*, Partial Differ. Equ. Appl. **8** (2023) 100592.

- [2] R. Choudhary, D. Kumar, S. Singh, *Second-order convergent scheme for time-fractional partial differential equations with a delay in time*, J. Math. Chem. **61** (2023) 21–46.
- [3] R. Choudhary, S. Singh, D. Kumar, *A second-order numerical scheme for the time-fractional partial differential equations with a time delay*, Comput. Appl. Math. **41** (2022) 114.
- [4] I.T. Daba, G.F. Duressa, *Extended cubic B-spline collocation method for singularly perturbed parabolic differential-difference equation arising in computational neuroscience*, Int. J. Numer. Method. Biomed. Eng. **37** (2021) e3418.
- [5] F.W. Gelu, G.F. Duressa, *A uniformly convergent collocation method for singularly perturbed delay parabolic reaction-diffusion problem*, Abstr. Appl. Anal. **2021** (2021) 8835595 .
- [6] C.A. Hall, *On error bounds for spline interpolation*, J. Approx. Theory **1** (1968) 209–218.
- [7] M.K. Kadalbajoo, P. Arora, *Fitted Collocation Method for Convection-diffusion Problems with Two Small Parameters*, Neural, Parallel Sci. Comput. **20** (2012) 133–152.
- [8] I. Karatay, N. Kale, S. Bayramoglu, *A new difference scheme for time fractional heat equations based on the Crank-Nicholson method*, Fract. Calc. Appl. Anal. **16** (2013) 892–910.
- [9] D. Kumar, P. Kumari, *A parameter-uniform numerical scheme for the parabolic singularly perturbed initial boundary value problems with large time delay*, J. Appl. Math. Comput. **59** (2019) 179–206.
- [10] K.P. Kumar, J. VigoAguiar, *Numerical solution of time-fractional singularly perturbed convection-diffusion problems with a delay in time*, Math. Methods Appl. Sci. **44** (2021) 3080–3097.
- [11] X. Liu, M. Abbas, H. Yang, X. Qin, T. Nazir, *Novel finite point approach for solving time-fractional convection-dominated diffusion equations*, Adv. Differ. Equ. **2021** (2021) 4.
- [12] E.A. Megiso, M.M. Woldaregay, T.G. Dinka, *Fitted Tension Spline Method for Singularly Perturbed Time Delay Reaction Diffusion Problems*, Math. Probl. Eng. **2022** (2022) 8669718 .
- [13] S.T. Mohyud-Din, T. Akram, M. Abbas, A.I. Ismail, N.H. Ali, *A fully implicit finite difference scheme based on extended cubic B-splines for time fractional advection-diffusion equation*, Adv. Differ. Equ. **2018** (2018) 109 .
- [14] H. Naz, T. Dumrongpokaphan, T. Sitthiwiratham, H. Alrabaiah, K.J. Ansari, *A numerical scheme for fractional order mortgage model of economics*, Results Appl. Math. **18** (2023) 100367.
- [15] N.T. Negero, G.F. Duressa, *Uniform convergent solution of singularly perturbed parabolic differential equations with general temporal-lag*, Iran. J. Sci. Technol. Trans. Sci. **46** (2022) 507–524.
- [16] N.T. Negero, G.F. Duressa, *A method of line with improved accuracy for singularly perturbed parabolic convection-diffusion problems with large temporal lag*, Results Appl. Math. **11** (2021) 100174.

- [17] N.T. Negero, G.F. Duressa, *Parameter-uniform robust scheme for singularly perturbed parabolic convection-diffusion problems with large time-lag*, *Comput. Methods Differ. Equ.* **10** (2022) 954–968.
- [18] F.A. Rihan, *Computational methods for delay parabolic and timefractional partial differential equations*, *Numer. Methods Partial Differ. Equ.* **26** (2010) 1556–1571.
- [19] M. Sarboland, *Numerical solution of time fractional partial differential equations using multi quadric quasi-interpolation scheme*, *Eur. J. Comput. Mech.* **27** (2018) 89–108.
- [20] V. Saw, S. Kumar, *Collocation method for time fractional diffusion equation based on the Chebyshev polynomials of second kind*, *Int. J. Appl. Comput. Math.* **6** (2020) 117.
- [21] M. Stynes, E. O’Riordan, J.L. Gracia, *Error analysis of a finite difference method on graded meshes for a time-fractional diffusion equation*, *SIAM J. Numer. Anal.* **55** (2017) 1057–1079.
- [22] N.H. Sweilam, M.M. Khader, A.M. Mahdy, *Crank-Nicolson finite difference method for solving time-fractional diffusion equation*, *J. Fract. Calc. Appl.* **2** (2012) 1–9.
- [23] S.K. Tesfaye, M.M. Woldaregay, T.G. Dinka, G.F. Duressa, *Fitted computational method for solving singularly perturbed small time lag problem*, *BMC Res. Notes.* **15** (2022) 318.
- [24] Y. Ucar, N.M. Yagmurlu, O. Tasbozan, A. Esen, *Numerical solution of some fractional partial differential equations using collocation finite element method*, *Prog. Fract. Differ. Appl.* **1** (2015) 157–164.
- [25] J.M. Varah, *A lower bound for the smallest singular value of a matrix*, *Linear Algebra Appl.* **11** (1975) 3–5.
- [26] M.M. Woldaregay, W.T. Aniley, G.F. Duressa, *Novel numerical scheme for singularly perturbed time delay convection-diffusion equation*, *Adv. Math. Phys.* **2021** (2021) 6641236 .
- [27] M. Yaseen, M. Abbas, M.B. Riaz, *A collocation method based on cubic trigonometric B-splines for the numerical simulation of the time-fractional diffusion equation*, *Adv. Differ. Equ.* **2021** (2021) 210.